SCIENCE AND TECHNOLOGY ORGANIZATION
CENTRE FOR MARITIME RESEARCH AND EXPERIMENTATION

Reprint Series CMRE-PR-2013-006

Benefit assessment of glider adaptive sampling in the Ligurian Sea

Baptiste Mourre, Alberto Alvarez

January 2014

Originally published in:

Deep-Sea Research I, Vol 68, 2012, pp. 68-78.

About CMRE

The Centre for Maritime Research and Experimentation (CMRE) is a world-class NATO scientific research and experimentation facility located in La Spezia, Italy.

The CMRE was established by the North Atlantic Council on 1 July 2012 as part of the NATO Science & Technology Organization. The CMRE and its predecessors have served NATO for over 50 years as the SACLANT Anti-Submarine Warfare Centre, SACLANT Undersea Research Centre, NATO Undersea Research Centre (NURC) and now as part of the Science & Technology Organization.

CMRE conducts state-of-the-art scientific research and experimentation ranging from concept development to prototype demonstration in an operational environment and has produced leaders in ocean science, modelling and simulation, acoustics and other disciplines, as well as producing critical results and understanding that have been built into the operational concepts of NATO and the nations.

CMRE conducts hands-on scientific and engineering research for the direct benefit of its NATO Customers. It operates two research vessels that enable science and technology solutions to be explored and exploited at sea. The largest of these vessels, the NRV Alliance, is a global class vessel that is acoustically extremely quiet.

CMRE is a leading example of enabling nations to work more effectively and efficiently together by prioritizing national needs, focusing on research and technology challenges, both in and out of the maritime environment, through the collective Power of its world-class scientists, engineers, and specialized laboratories in collaboration with the many partners in and out of the scientific domain.

NOTE: The CMRE Reprint series reprints papers and articles published by CMRE authors in the open literature as an effort to widely disseminate CMRE products. Users are encouraged to cite the original article where possible.

Deep-Sea Research I 68 (2012) 68–78

Contents lists available at SciVerse ScienceDirect

Deep-Sea Research I

journal homepage: www.elsevier.com/locate/dsri

Instruments and Methods

Benefit assessment of glider adaptive sampling in the Ligurian Sea

Baptiste Mourre*, Alberto Alvarez

NURC, Viale San Bartolomeo 400, La Spezia, Italy

ARTICLE INFO

Article history:
Received 18 January 2012
Received in revised form
14 May 2012
Accepted 20 May 2012
Available online 21 June 2012

Keywords:
Glider
Adaptive sampling
Operational ocean prediction
Super-ensemble
Ligurian Sea

ABSTRACT

The benefits of piloting a glider during a 6-day period via an adaptive sampling procedure in a $80 \times 60\ km^2$ marine area are assessed under a fully operational framework. The glider trajectory was adapted to reduce the ocean temperature uncertainties predicted by the operational 3-D super-ensemble model in the Ligurian Sea in August 2010. Two sets of real time model predictions are compared, which assimilate observations from (1) the adaptive-sampling-driven glider and (2) an independent glider flying in the same area. The piloting algorithm was able to successfully guide the glider along the planned trajectories. These were nevertheless not fully completed due to un-predicted adverse currents faced along the transects. Despite operational constraints and model prediction errors, the adaptive sampling procedure is shown to meet the proposed objective, i.e. a reduction of the 48-h model temperature uncertainty predicted in the upper 200 m. Moreover, measurements collected during the last 48-h forecast cycle from (i) an ocean mooring, (ii) a repeated *ScanFish* transect and (iii) more irregularly distributed platforms, all indicate that the actual prediction error is lower in the simulation assimilating the data from the adaptive sampling. Quantitatively, the total root-mean-square error is reduced by 18% at the end of the field experiment in comparison with the control simulation.

1. Introduction

Autonomous Underwater Vehicles (AUVs) have a recognized potential to greatly improve our observing capability in the complex and rapidly evolving coastal ocean (Curtin et al., 1993). Equipped with Conductivity-Temperature-Depth (CTD) sensors, AUV platforms are able to provide sustained observations over vast ocean regions. In addition, AUVs allow high horizontal and vertical sampling resolutions, making them able to detect small scale features which characterize coastal environments. Underwater gliders are a type of AUVs that use their hydrodynamic shape and small buoyancy changes to induce net horizontal motions in the water column. This low-power propulsion procedure provides gliders with long endurance and autonomy at sea, which makes them key elements of Coastal Ocean Observatories throughout the world (e.g. US Integrated Ocean Observing System-IOOS, Australian Integrated Marine Observing System-IMOS).

A few examples in the literature have demonstrated the potential of glider data at the regional scale. Davis et al. (2008) showed how glider data could give new insights into the description of physical and biological fronts in the southern California Current System. Castelao et al. (2008) provided a detailed characterization of the spatial scales of ocean dynamics variability in the central Middle Atlantic Bight using high-resolution glider observations. The arrival of El Niño effects off California's coast was recently revealed by glider observations (Todd et al., 2011). The complementarity between self-propelling gliders and other observational platforms has also been documented. Ruiz et al. (2009) and Bouffard et al. (2010) highlighted the synergy between glider observations and sea level altimeter data to characterize the coastal and mesoscale dynamics in the Balearic Sea. From a methodological point of view, Alvarez and Reyes (2010) proposed a functional model to merge glider-like observations and remote-sensing measurements to improve volumetric temperature estimations in coastal regions. Finally, synergies between gliders and ocean models are currently being exploited in operational ocean forecast systems (e.g. Chao et al., 2008, 2009; Zhang et al., 2010a; Dobricic et al., 2010).

Glider missions are typically planned to reach a series of locations commonly called waypoints. The possibility of freely selecting the mission waypoints, so that the data are collected at optimal locations to maximize their information content, has led to the concept of glider adaptive sampling. The general concept of adaptive sampling is defined in Lermusiaux (2007) as the problem of "predicting the types and locations of observations that are expected to be most useful, based on given estimation objectives and the constraints of the available assets". Examples of *estimation objectives* include the improvement of the description of a

* Corresponding author. Tel.: +39 018 752 7215; fax: +39 018 752 7700.
E-mail address: mourre@nurc.nato.int (B. Mourre).

0967-0637/$ - see front matter © 2012 NATO Undersea Research Centre. Published by Elsevier Ltd. All rights reserved.
http://dx.doi.org/10.1016/j.dsr.2012.05.010

particular local oceanic process, the optimization of the data coverage over a specific region, or the reduction of model uncertainties after data assimilation. The two main *constraints of the available assets* in the case of ocean gliders are the time available for the glider mission and the oceanic currents, which may limit the control on the vehicle and prevent it from reaching the planned locations.

The need for optimal sampling methodologies for ocean gliders was pointed out in the 1990s by Curtin et al. (1993) and Robinson and Glenn (1999). Techniques for optimal path planning of AUVs were then improved by considering the influence of ocean currents (Alvarez et al., 2004), the coordinated control of multi-platforms (Fiorelli et al., 2004; Leonard et al., 2006), the complexification of the cost-function (Heaney et al., 2007) and alternative Mixed Integer Linear Programming methods (Yilmaz et al., 2008). Glider control experiments were successfully carried out at sea using these improved techniques (Wang et al., 2009; Leonard et al., 2010). Algorithms that generate optimal glider paths based on predictions of regional ocean models were also recently developed, either by tracking an evolving feature (Smith et al., 2010), or by exploiting the expected spatio-temporal influence of observations (Zhang et al., 2010b). The Monterey Bay was the theater of two large multi-institution experiments in 2003 (AOSN-II: Second Autonomous Ocean Sampling Network Experiment) and 2006 (ASAP: Adaptive Sampling and Prediction Experiment), which demonstrated the viability of adaptive sampling methodologies in the coastal ocean based on the predictions of real time data-assimilative models (Ramp et al., 2009, 2011; Haley et al., 2009).

Since operational constraints related to platform motion limitations, model inaccuracies, algorithm computing time or human factors may limit the efficiency of the adaptive sampling procedure in real situations, the evaluation of the benefits of guiding gliders towards preferred locations in real at-sea scenarios are now necessary to validate the demonstrated adaptive sampling procedures. This paper presents such an evaluation in the framework of the Recognized Environmental Picture experiment carried out in the Ligurian Sea (Western Mediterranean) in August 2010 (hereafter REP10). A large number of observation platforms were deployed at sea from the NATO research vessel N/RV Alliance. These include gliders, CTD stations, a shipborne surface CTD and a CTD onboard a towed undulating *ScanFish* vehicle. This extensive collection of *in situ* measurements provides a valuable dataset for the validation of model ocean temperature predictions.

The *estimation objective* defined to guide the adaptive sampling procedure in this study consists in minimizing the uncertainty associated with the operational 3-D super-ensemble (3DSE, Lenartz et al., 2010) temperature predictions in the upper 200 m of the water column in a 80×60 km^2 restricted area offshore La Spezia, Italy. The 3DSE method, which optimally combines multiple model forecasts after confrontation to observations during a recent learning period, was shown to improve ocean temperature prediction skills when a sufficient data collection was carried out during the recent past (Lenartz et al., 2010; Mourre et al., 2012). The 3DSE method provides an associated uncertainty estimate which was shown to have a proper consistency with the observed model-data mismatch, yet with a tendency towards underestimation (Mourre et al., 2012). The 3DSE data assimilative operational model was run at NURC during the experiment, and was naturally selected to carry out this adaptive sampling exercise.

The assessment of benefits, if any, of adaptive sampling in a fully operational framework is done by confronting the forecast skill of the 3DSE model when assimilating data from a glider guided by the model uncertainty with the prediction skill obtained when data comes from a glider following an independent trajectory.

The paper is articulated as follows. Section 2 presents the REP10 experiment, the 3DSE method and the glider mission planning procedure used for the adaptive sampling. The benefits of the real time glider adaptive sampling experiment are evaluated in Section 3. Finally, Section 4 concludes the paper.

2. Model and data

2.1. REP10 sea trial

The REP10 experiment was carried out in the Ligurian Sea from 19 August to 3 September, 2010. An extensive set of *in situ* observations was collected, with the purpose to improve the rapid characterization of the marine environment. During a 2-week period, the N/RV Alliance was used to collect ocean temperature and salinity measurements through a continuous shipborne surface CTD, a CTD housed onboard a towed undulating *ScanFish* vehicle and CTD profiles at fixed stations. In addition, four *SLOCUM* underwater gliders equipped with CTDs were deployed to profile the upper 200 m of the sea. These shallow water gliders were identified with the following names: *GRETA*, *LAURA*, *ZOE* and *NATALIE*. A deep-diving *SPRAY* glider was also deployed to provide oceanic conductivity and temperature data from the surface to 1000 m depth. Finally, an Ocean Data Acquisition System (ODAS Italia 1 mooring) provided temperature time series at 43.84°N 9.11°E for five discrete levels from the surface to 36 m depth. The REP10 temperature dataset is used to validate the adaptive sampling exercise, which was restricted in both space and time with respect to the whole REP10 sea trial extent. Specifically, the adaptive sampling experiment was performed from 20 to 28 August 2010, in a limited 80×60 km^2 area offshore La Spezia, Italy.

The satellite sea surface temperature (SST) measured in the Ligurian Sea by the Advanced Very High Resolution Radiometer (AVHRR—NOAA TIROS-N) on 22 August 2010 is illustrated in Fig. 1, together with the boundaries of the adaptive sampling area and all REP10 temperature *in situ* observations collected from 22

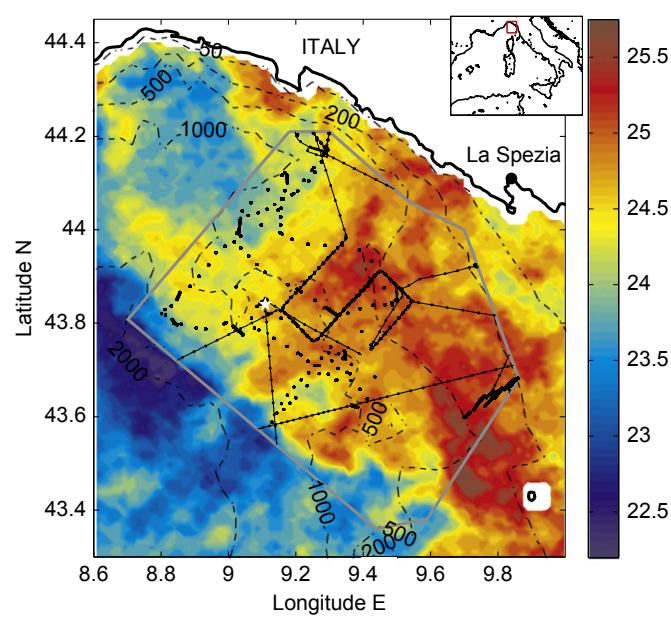

Fig. 1. Sea surface temperature (°C) measured by the Advanced Very High Resolution Radiometer onboard NOAA satellite on 22 August 2010 at 08:10. Dashed contours indicate the position of the isobaths. The adaptive sampling area is delimited by the gray polygon. Inside this area, the black dots illustrate the position of REP10 observations collected between 22 August 18:00 and 28 August 18:00 from the surface to 200 m depth, the solid lines show the N/RV Alliance ship track and the white star at 43.84°N 9.11°E represents the position of the ODAS Italia 1 mooring.

to 28 August and available for validation. The region is characterized by a surface temperature front separating the coastal waters from the colder waters present offshore over the deep ocean, with SST gradients up to 2 °C per 10 km. Submesoscale structures develop in the frontal zone. Relatively cold surface waters are also found north of 44°N and west of 9.1°E associated with the narrowing of the shelf and the curvature of the 1000 m isobath towards the coast. Notice that validation measurements were mainly collected in the warm side of the front. However, some observations taken in the vicinity of the boundaries of the adaptive sampling area may have a signature of the colder water intrusions induced by the frontal variability.

2.2. REP10 operational modelling

The 3DSE (Lenartz et al., 2010) was run operationally during the sea trial experiment to provide daily 48-h ocean temperature forecasts. 3DSE aims to provide an improved consensual ocean forecast when multiple numerical predictions and data are available. Models are combined through optimal weighting over a given oceanic domain, with the possibility for the model weights to vary in space. *A priori* spatial weight error correlations are used to update model weights in non-observed areas. The operational implementation uses a 48-h past learning period to adjust model weights through a least-square estimation approach. The optimal weights are then used to combine individual predictions for the next 48 h.

Three high-resolution ocean models were used in the current implementation of the 3DSE. The first operational ocean forecasting system was run at the US Naval Research Laboratory NRL-SSC, based on the Navy Coastal Ocean Model (NCOM) (Martin, 2000) coupled to the Navy Coupled Ocean Data Assimilation module (NCODA) (Cummings, 2005). The second system was the French PREVIMER system (http://www.previmer.org), which provides ocean forecasts over the north-western Mediterranean Sea with MARS3D (Lazure and Dumas, 2008) as the core ocean model. The third system, run at the NATO Undersea Research Centre (NURC), is based on the ROMS ocean model (Haidvogel et al., 2008), with a setup dedicated to the REP10 sea trial framework. All three models have a horizontal resolution around 1.5 km. The resolution of the common grid defined to run the 3DSE is 3 km in the horizontal direction, and 10 m in the vertical.

Data from the Operational Sea Surface Temperature and Sea Ice Analysis (OSTIA) (Stark et al., 2007), describing the daily observed surface ocean temperature conditions, were assimilated during the 3DSE learning period, together with glider observations. High frequency measurements from the gliders were preprocessed to filter out the shortest scales. More specifically, glider observations were interpolated on the vertical model grid so as to remove the vertical variability at scales smaller than the model resolution. Moreover, a real time quality check was applied to remove potential out-of-range values in the real time glider CTD dataset. The total observation error gathering both the instrumental noise and the representativity error was estimated to have a standard deviation of 0.8 °C and 0.4 °C for OSTIA data and *in situ* glider observations, respectively.

Gaussian correlations based on the distance between two gridpoints were used as initial spatial weight error correlations. Horizontal and vertical decorrelation distances were fixed to 50 km and 20 m, respectively. Weight error variances were initialized with a homogeneous value of 0.01. The 3DSE model was run recursively, meaning that *a posteriori* model weights and associated error covariances after a given analysis were used to initialize the subsequent simulation. Further details about the present 3DSE implementation can be found in Mourre et al. (2012).

The ocean velocity predictions that are needed for the glider mission planning were deduced from an independent 3DSE simulation. In the absence of ocean velocity observations (notice that velocities inferred from the drift of the gliders were not assimilated), and given the current univariate operational implementation of the 3DSE, these predictions were only the average ocean velocities forecasted by the three input ocean models.

2.3. REP10 mission planning of gliders

The glider mission planning procedure implemented in this experiment is detailed in Alvarez and Mourre (2012), in which different optimal criteria to be potentially used for the adaptive sampling of a glider in the presence of a mooring were evaluated through Observing System Simulation Experiments. The main characteristics of the procedure are summarized here for completeness. The procedure attempts to provide an optimal glider trajectory for specified mission parameters. These parameters are the area of operation, the mission time T_M, the current glider position $\overrightarrow{x_0}$ and nominal speed V, the navigation time T_S between two surfacings of the glider and T_W between two successive waypoints, the vertically averaged model ocean velocity prediction (the average is performed from the surface to the maximum glider diving depth, i.e. 200 m), the vertically averaged model temperature prediction and associated error covariances. The glider mission time T_M is 48 h in this experiment. A glider trajectory compatible with mission constraints is defined by a sequence of waypoints: $\Gamma = \{\overrightarrow{x_0}, \overrightarrow{x_1}, \ldots, \overrightarrow{x_M}\}$. The glider must cover Γ in T_M, and each segment $\{\overrightarrow{x_i}, \overrightarrow{x_{i+1}}\}_{i=1}^{M}$ in T_W. Surfacing occurs at time intervals determined by T_S, resulting in a total of T_W/T_S surfacing locations per segment. At each surfacing, the glider corrects its heading according to (i) its actual position and (ii) the estimation of the local oceanic current field deduced from the mismatch between the planned and actual positions of the platform. The 48-h average oceanic currents predicted by the model are used to estimate the glider trajectory between two waypoints given the time T_W and the glider nominal speed V. This procedure aims to generate glider trajectories which are theoretically timely reachable by the platform. In reality, inaccuracies in ocean velocity predictions may prevent the planned trajectory from being properly completed. A least-square optimal estimation (also known as objective analysis or Gauss–Markov smoothing) (McIntosh, 1990; Stein, 1999) is performed to generate the temperature field estimate and the associated uncertainty corresponding to a given realistic glider trajectory. *A priori* errors used as input for the objective analysis are provided by the 48-h average temperature error covariances of the model prediction. The full set of equations used in this adaptive sampling strategy is presented in Alvarez and Mourre (2012).

A Pattern Search Optimization (PSO) algorithm (Hooke and Jeeves, 1961) is implemented to find the optimal solution among the possible glider trajectories. Alternative minimization approaches using either a Genetic Algorithm or the Simulated Annealing were found to require longer convergence times. As a consequence, PSO was considered as the most suitable algorithm to be applied in our operational framework.

Finally, an optimality criterion needs to be selected to define the "best" possible glider trajectory. If adaptive sampling procedures define the optimal trajectory as the one leading to "the smallest" *a posteriori* error covariance matrix, a scalar measure of the "smallness" of the matrix still needs to be defined. The trace, the maximum diagonal value, or the maximum eigenvalue of the error covariance matrix may be considered here. Since the different criteria may lead to different optimal glider trajectories, all other inputs remaining constant, the evaluation of the performance of the different designs is of particular interest. Such an

evaluation was carried out in Alvarez and Mourre (2012) for a glider-mooring observing network, showing that the so-called A-optimal design, which considers the trace of the error covariance matrix as the quantity to be minimized, yielded the best results. Based on this evaluation, and on the results of more specific Observing System Simulation Experiments (OSSEs) performed in the REP10 operational framework (not shown here), the A-optimality criterion was selected for the operational exercise.

3. Benefit assessment of glider adaptive sampling during REP10

3.1. Methodology

Four *SLOCUM* shallow water gliders and one *SPRAY* deep-sea glider were flying in the restricted oceanic area illustrated in Fig. 1 from 20 to 28 August. Two of the shallow water gliders (*GRETA* and *LAURA*) were dedicated to the adaptive sampling exercise, while the remaining three platforms (*NATALIE*, *ZOE* and *SPRAY*) were specifically used for independent validation purposes.

For what concerns adaptive sampling, glider *GRETA* executed three 48-h programming cycles from 20 to 26 August guided by the uncertainty field of the 3DSE forecasts. The glider mission planning was performed for three different dates t_0 (20, 22 and 24 August at 18:00), providing the optimal *GRETA* trajectory for the next 48 h. This planning was based on (i) the mean depth-averaged 3DSE temperature and associated uncertainty predicted for the next 48 h, (ii) the mean depth-averaged 3DSE ocean currents predicted for the next 48 h and (iii) the practical mission constraints described in Section 2.3. After the execution of the mission planner, the glider was programmed to visit the sequence of optimal waypoints from t_0 to t_0+48 h. The temperature data collected by the glider CTD were then assimilated in the subsequent 3DSE simulation (i.e. used for the 3DSE learning phase) run at t_0+48 h. The resulting 3DSE prediction, valid from t_0+48 h to t_0+96 h, provided updated inputs to the following mission planner executed at t_0+48 h. The succession of glider mission planning and 3DSE cycles performed between 20 and 28 August is represented diagrammatically in Fig. 2. The elapsed times required for the 48-h 3DSE forecast computation and successive glider path optimization were 25 and 30 min, respectively. The

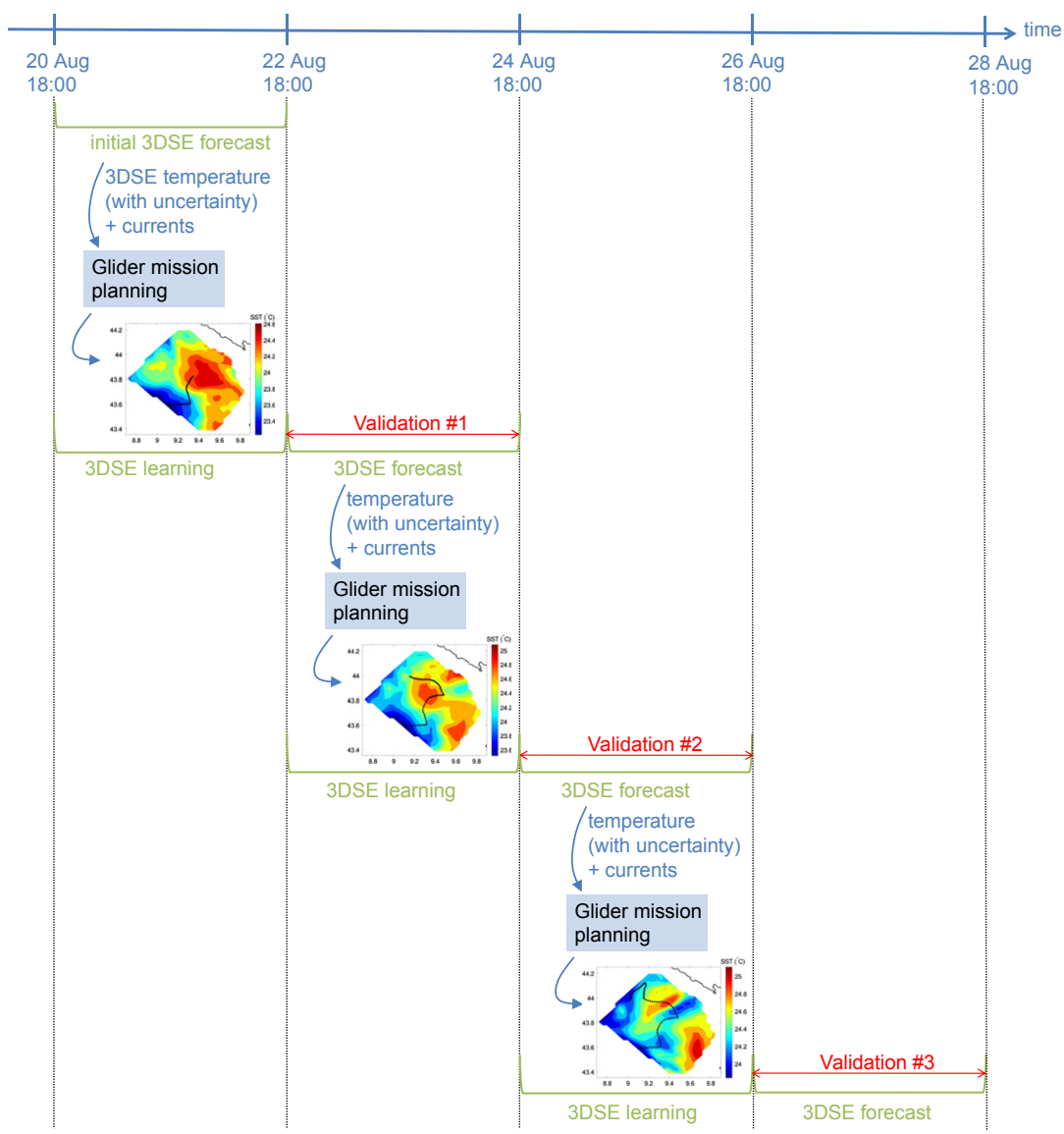

Fig. 2. Succession of glider mission planning and 3DSE cycles performed between 20 and 28 August.

glider was left during about 1 h in a parking position close to the surface waiting for the new instructions during this computation period.

Concurrently, glider *LAURA* was operated in the same area to perform a mission unrelated to the 3DSE uncertainty. The corresponding trajectory, which is characterized by a relative dense coverage of the frontal zone, provides one realization of the many possible non-optimal trajectories (regarding our particular optimization criterion) that a glider could follow in the selected area. By oversampling a particular zone close to the thermal front, this trajectory likely represents a bad case with regard to the A-optimality criterion which generally leads to more geographically uniform sampling strategies (Alvarez and Mourre, 2012). However, it also provides a better monitoring of the frontal area, where the variability is expected to be the largest. The data collected from this second glider were used to train a second set of independent 3DSE runs. The 3DSE predictions obtained after assimilation of *GRETA* observations were compared to these alternative predictions to assess the benefits of adaptive sampling. In the following, 3DSE-GRETA and 3DSE-LAURA will be used to refer to the 3DSE simulations assimilating *GRETA* and *LAURA* observations, respectively (i.e. adaptive-sampling-driven and control simulations, respectively). Notice that the OSTIA analyzed SST data were assimilated in both cases.

The forecast validation was carried out during the three 48-h forecast periods based on independent REP10 data from *SPRAY*,

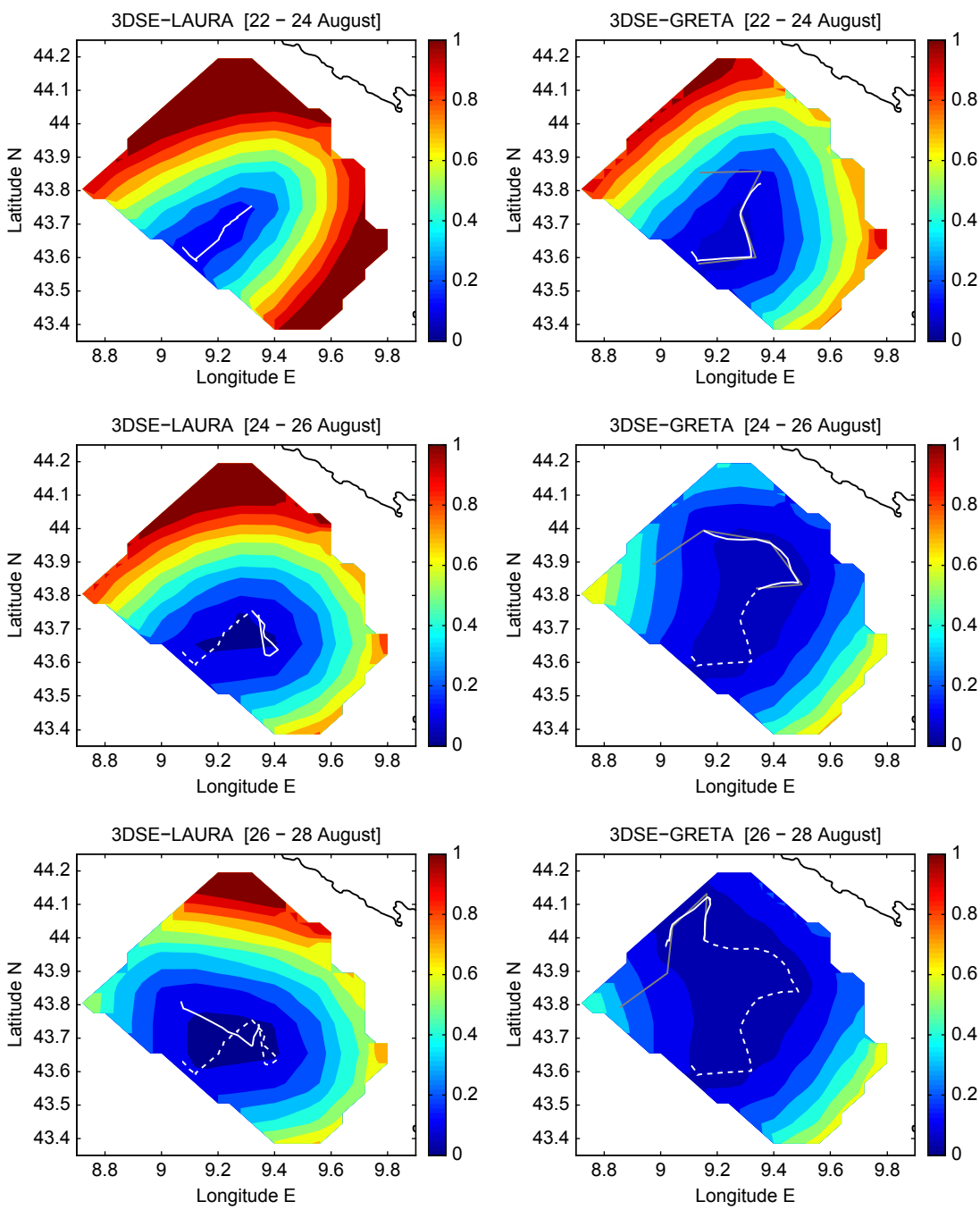

Fig. 3. Depth-integrated 48-h-average temperature uncertainty forecasts (°C) from 3DSE-LAURA (left panels) and 3DSE-GRETA (right panels) for the three validation periods. The solid white lines show the real glider trajectories during the 48 h previous to the period under concern (t_0-48 h to t_0). In the right panels, the solid gray lines illustrate the planned trajectories. The dashed white lines represent the real glider trajectories completed before the last glider mission planning (t_0-144 h to t_0-48 h).

NATALIE and *ZOE* gliders, CTD stations, the ship surface CTD and the CTD onboard the undulating *ScanFish* vehicle. Temperature data were first interpolated on the vertical 3DSE model grid to limit the impact of representativity errors on the validation results.

3.2. Results

3.2.1. Uncertainty forecasts

The depth-averaged (from the surface to 200 m depth) 48-h mean 3DSE uncertainty forecasts obtained from 3DSE-GRETA and 3DSE-LAURA are represented in Fig. 3. The planned (solid gray lines) and actual (solid white lines) glider trajectories between 20 and 26 August are also displayed in the figure.

Glider *GRETA* is first sent towards the north-east, then directed north-westwards during the second cycle, and finally piloted southwards when it approaches the domain boundary during the last cycle. The objective consisting in minimizing the mean value of the uncertainty over the whole domain generates an optimal trajectory which avoids redundant measurements. The glider is guided towards locations which are the most remote as possible to previously visited places. A rough estimate of the time period of influence of the assimilated glider observations in the model could be provided by the synoptic time scale estimated in this region from the NCOM model simulation in Alvarez and Mourre (2012), i.e. 4–5 days. Notice however that this estimate has to be considered with precaution since this time period of influence is also expected to vary with the time and position of the observations. The trajectory completed by glider *LAURA* differs in that the 6-day path intersects with itself, so that particular locations close to the frontal area are observed twice during the period of the experiment. Glider *LAURA* is directed north-eastwards during the first cycle, then south-eastwards during the first half of the second cycle, and finally north-westwards.

The good correspondence between the planned and real *GRETA* trajectories shows that the heading procedure, which re-directs the platform at each surfacing to correct for deviations from the planned position, has been working effectively at sea. However, the glider was found to be unable to cover more than three quarters of the total planned trajectories for the three periods under consideration. This limitation reveals the presence of unpredicted adverse currents faced along the glider transect. Fig. 4 illustrates the differences between the 48-h average predicted model currents, which are used in the glider mission planner, and the actual velocities estimated from the glider drift between successive surfacings. The time-averaged model velocity prediction exhibits significant errors in both direction and intensity during the three cycles. The time series of ocean velocities along the glider path (Fig. 4 panel d) shows that the differences between time-averaged and time-varying model velocities are weak compared to the differences between time-average model velocities and glider estimates along the platform trajectory. This indicates that the non-consideration of the temporal variability of model velocities in the mission planner is probably only a secondary source of error affecting the ocean velocity estimate in the planning procedure.

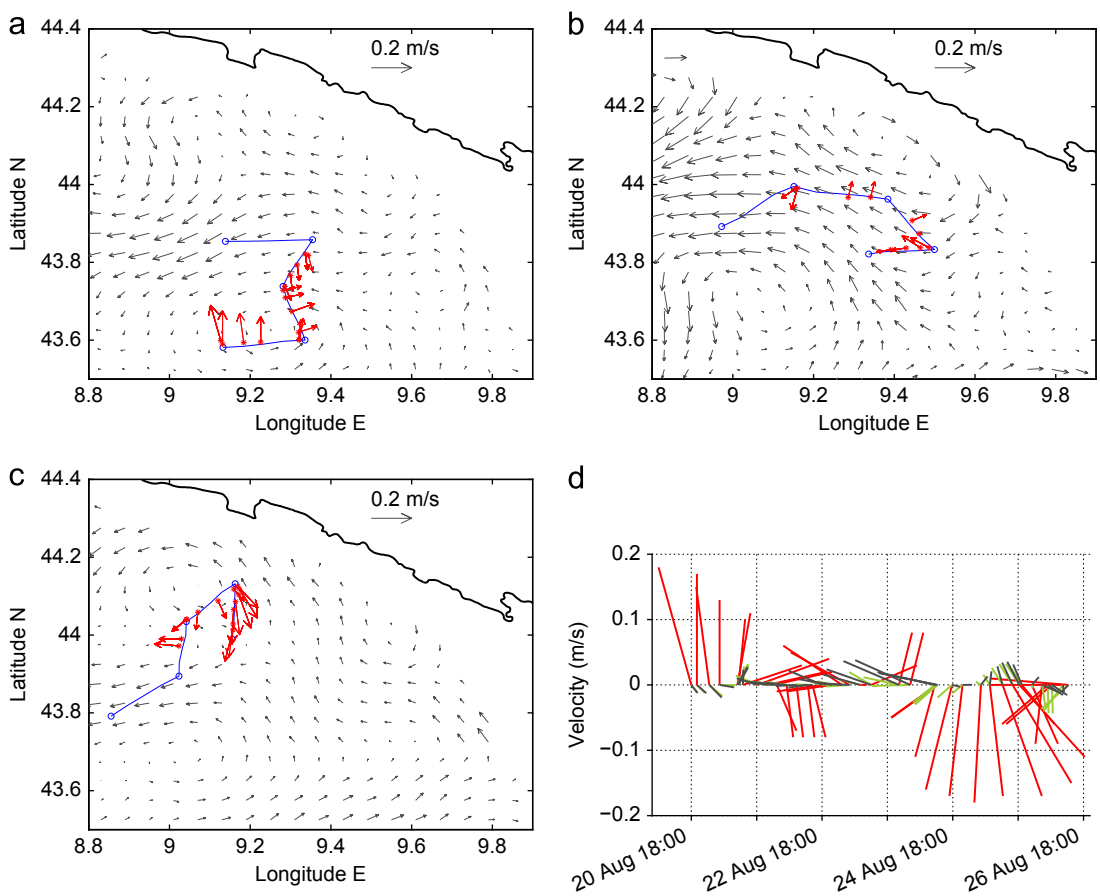

Fig. 4. Panels (a)–(c): mean surface-to-200 m depth-averaged ocean velocities predicted by the 3DSE model (gray arrows) for the periods (a) 20–22 August, (b) 22–24 August and (c) 24–26 August. The ocean velocities estimated from the glider drift are represented by the red arrows and the planned glider trajectories by the blue lines. Panel (d): depth-integrated velocity vectors (northward is up, eastward is right) along the 6-day glider path (in red: estimated from the glider drift, in gray: 48-h average 3DSE model prediction, in green: time-varying 3DSE model prediction). (For interpretation of the references to color in this figure caption, the reader is referred to the web version of this article.)

Table 1
Depth-integrated 48-h-averaged temperature uncertainty predicted by 3DSE-LAURA and 3DSE-GRETA.

Forecast period	Temperature uncertainty (°C)	
	3DSE-LAURA	3DSE-GRETA
22–24 August	0.76	0.51
24–26 August	0.55	0.25
26–28 August	0.42	0.19

The reduction of the 3DSE uncertainty along the glider trajectories can be appreciated in Fig. 3. The use of initial homogeneous and isotropic weight error correlations leads to a reduced uncertainty in the vicinity of the assimilated observations, and a gradual increase with the distance from them. This simply reflects the better confidence in the linear combination of ocean models by the 3DSE in the area where the model weights have been locally adjusted based on observations, than in the rest of the domain where the information has been propagated based on spatial correlation assumptions. The final 3DSE uncertainty is shown to be significantly reduced along the whole 6-day glider trajectory, which demonstrates that the recursive 3DSE uncertainty estimate is able to represent the cumulative impact of successive observations on the error reduction. Concerning glider *LAURA*, the limited geographical coverage of the sampling does not lead to a proper 3DSE uncertainty reduction in the northern edge of the domain. The predicted uncertainty exceeds 1 °C in this area. On the contrary, the adaptive path followed by glider *GRETA* results in a significant overall reduction of model uncertainty in the area of interest. The south-eastern edge of the domain, which is not visited by glider *GRETA* during the 6-day period, shows the largest uncertainty.

The depth-integrated average 3DSE temperature uncertainty predicted for the three validation periods for both assimilation scenarios are summarized in Table 1. In both cases the mean uncertainty decreases after each 48-h cycle. From the first cycle on, the adaptive-sampling-driven simulation leads to a lower mean uncertainty (0.51 versus 0.76 °C). During the last forecast period from 24 to 26 August, the average uncertainty obtained assimilating *GRETA* observations is 55% smaller than that assimilating *LAURA* data (0.19 versus 0.42 °C).

3.2.2. Measured forecast errors

Since model forecast uncertainty estimates may be inaccurate, it remains to be verified that the model temperature forecast error is actually reduced when assimilating the data from the adaptive sampling mission. In the following, model forecasts are evaluated against independent temperature observations collected from different platforms.

Fig. 5 illustrates the temporal series of ocean temperatures predicted by 3DSE-GRETA and 3DSE-LAURA at three different depths at the position of the ODAS mooring, together with the associated measurements. The thermocline is approximately located between 10 and 30 m depth in this area (see Fig. 7). Predictions at the surface (1 m depth) are similar in 3DSE-LAURA and 3DSE-GRETA during the whole simulation period due to the assimilation of OSTIA SST in both cases. Larger errors are found in the upper thermocline (12 m depth) where the variability is increased. During the first forecast cycle (0–48 h), and despite the position of *GRETA* and *LAURA* in the same area during the prior learning period (see Fig. 3 upper panel), significant differences are found between the two 3DSE predictions at 12 and 36 m depth, with 3DSE-GRETA better adjusted to the measurements. The detour to the east of glider *GRETA* during the learning period

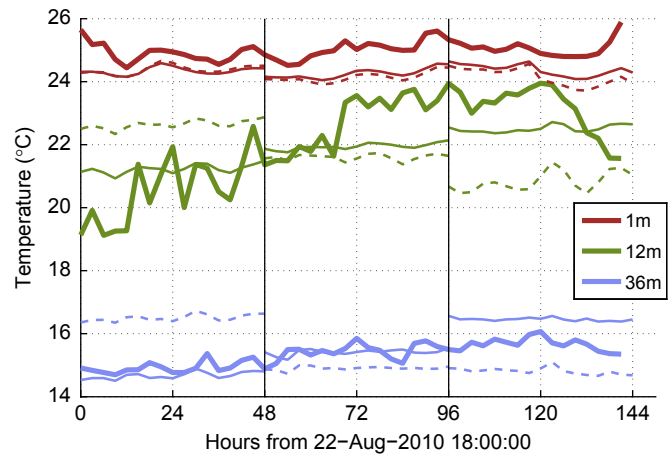

Fig. 5. Temporal series of temperature at 1 m, 12 m and 36 m depth at the ODAS Italia 1 mooring. 3DSE-LAURA forecasts are represented by the dashed thin lines, 3DSE-GRETA predictions by the solid thin line and observations by the solid thick line.

allowed to detect the presence of relatively colder waters, most probably by crossing some frontal intrusion as the one represented in Fig. 1 around 43.65°N 9.27°E. This did not happen with glider *LAURA*, which moved right towards warmer waters. The consequence is an overestimation of the predicted temperature by 3DSE-LAURA around the ODAS mooring. This overestimation is corrected during the second forecast cycle (48–96 h) after assimilation of the data collected from 22 to 24 August. 3DSE-GRETA is still in better agreement with observations during this second cycle. Notice however that none of the 3DSE simulations is able to reproduce neither the high-frequency variability in the thermocline, nor the particular warming event observed at 12 m depth around the 70-h forecast range. This highlights significant uncertainties in the challenging prediction of the thermocline by the input ocean models. The last cycle (96–144 hours) is characterized by a warming of 3DSE-GRETA prediction both in the thermocline and below, and a cooling of 3DSE-LAURA forecast in the thermocline compared to the previous cycle. These adjustments indicate that *GRETA* experienced warmer waters than expected during its last transect, while *LAURA* measured colder temperatures. Still, the forecast error of 3DSE-GRETA is lower than that of 3DSE-LAURA.

Fig. 6 compares the Root-Mean-Square Difference (RMSD) between observations and the 3DSE temperature predictions obtained from the two assimilation scenarios for the three 48-h verification cycles. The RMSD is computed independently for each observation sensor due to the diverse nature of the platforms involved and their spatial spreading. The location of the observations used during each validation period is displayed in the right panels to support the interpretation of the RMSD scores.

During the first forecast cycle, the prediction error of 3DSE-GRETA is lower than that of 3DSE-LAURA at ODAS buoy and along the *SPRAY* glider transect. At all other measurement locations, which are on average farther from both glider tracks, the error is lower for 3DSE-LAURA. This result, which is inconsistent with the uncertainty predictions presented in Fig. 3 and Table 1, where 3DSE-GRETA is expected to provide a lower uncertainty than 3DSE-LAURA, indicates significant inaccuracies in the 3DSE prediction and its associated uncertainty estimate outside the area spanned by the assimilated observations. The spatial extrapolation of the information from the location of assimilated observations to the rest of the domain remains a weakness of the 3DSE method when a limited number of observations is considered. Notice that the significant variability of the RMSD magnitudes is

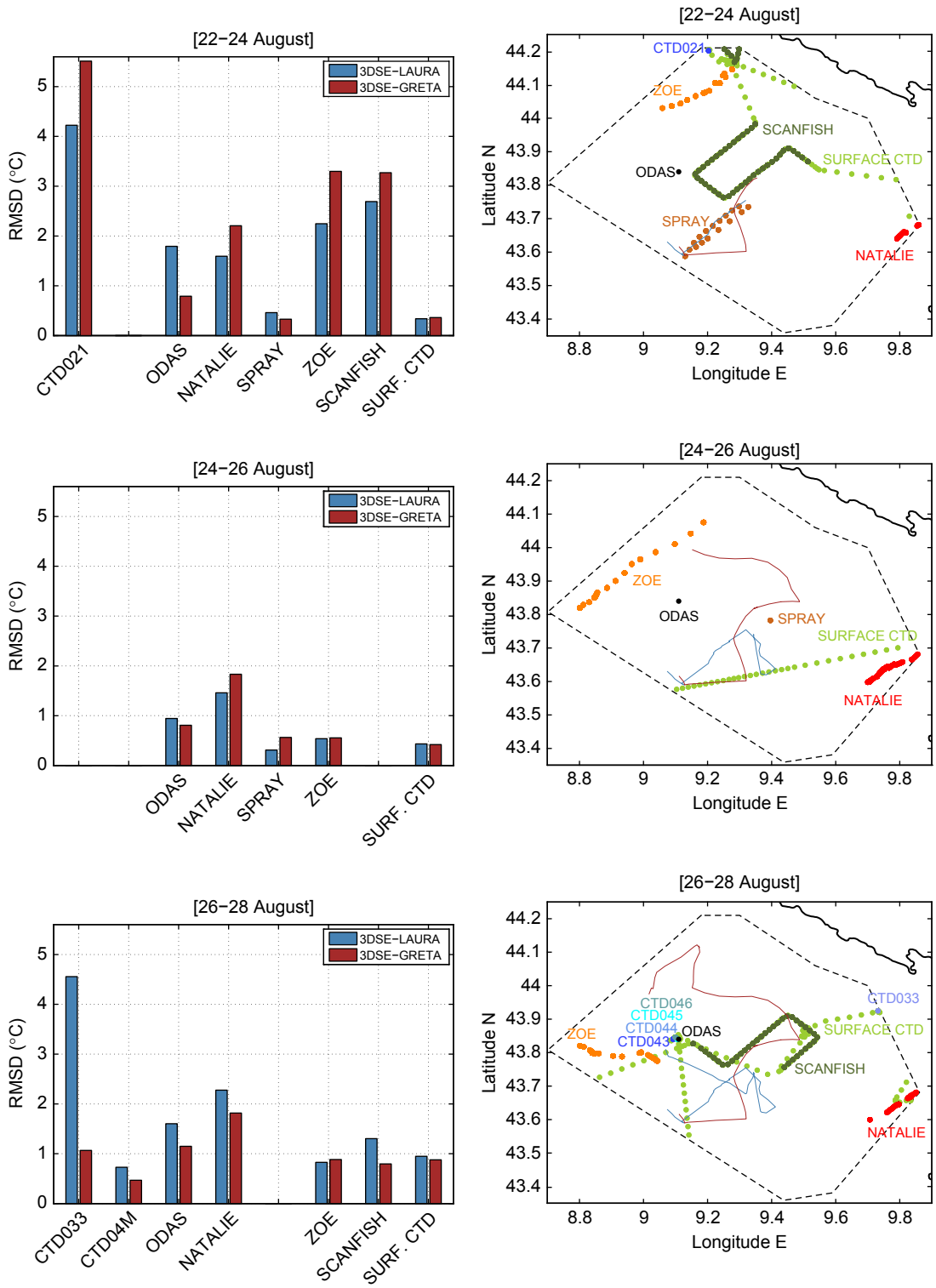

Fig. 6. Left: root-mean-square differences between 3DSE temperature predictions and observations for the three forecast validation periods. Right: position of observations used for the validation. LAURA and GRETA glider tracks prior to the illustrated validation period are plotted as blue and red solid lines, respectively. In the bottom left diagram, the label CTD04M gathers the four CTDs CTD043 to CTD046, which were collected at very close locations. (For interpretation of the references to color in this figure caption, the reader is referred to the web version of this article.)

mainly due to the diversity of the measurement depth range between the different platforms, given that the prediction error significantly varies along the vertical, with larger values in the thermocline, as shown in Fig. 5. CTD021 profiled the ocean from 10 to 80 m, the *ScanFish* from 2 to 70 m, *ZOE* and *NATALIE* from the surface to 180 m and the *SPRAY* glider from 10 to 200 m. At the surface, ship CTD measurements indicate similar performance of both 3DSE predictions, as observed at the ODAS mooring (Fig. 5).

During the second forecast cycle, the adaptive-sampling-driven simulation provides a lower RMSD compared to the alternative prediction at the ODAS mooring. The 3DSE prediction error along the transect of glider *ZOE* is similar in 3DSE-GRETA and

3DSE-LAURA. A more detailed analysis shows that the RMSD against the north-easternmost *ZOE* observations (north of 43.95°N, i.e. the closest to *GRETA* track) is lower in 3DSE-GRETA than in 3DSE-LAURA, while it is the opposite south of 43.95°N. Notice that *ZOE* data were collected in the vicinity of the thermal front and contains the signature of the associated submesoscale variability, which is not accurately represented in the model. The prediction error is lower in 3DSE-LAURA when compared to the *SPRAY* glider, which position is close to the most recent *LAURA* data. Away from the area of *GRETA* and *LAURA* observations, measurements collected by glider *NATALIE* reveal a slightly better performance of 3DSE-LAURA over 3DSE-GRETA. However, the RMSD is large in both cases due to the significant distance between these measurements and the assimilated observations. Again, RMSD scores are similar at the surface.

The benefit of the adaptive sampling procedure appears more clearly during the last forecast cycle when the predictions are impacted by the whole 6-day sampling period and when the validation dataset is also improved. The RMSD scores against all observation sources except glider *ZOE*, which is moving in the frontal area, are significantly reduced when considering the adaptive-sampling-driven simulation. Performances are similar in the case of *ZOE* data. Notice that CTD033 only provided measurements in the surface layer between 0 and 30 m, which explains the magnitude of the associated RMSD values. CTD043 to CTD046 went down to 200 m. The total RMSD considering all observation sources during this last cycle is reduced by 18% in 3DSE-GRETA compared to 3DSE-LAURA (1.08 versus 1.32 °C). The repetition of *ScanFish* measurements along a transect with similar characteristics as the one carried out during the first forecast cycle allows to show the improvement of the model prediction in the central part of the domain due to the 6-day adaptive sampling trajectory. While 3DSE-LAURA outperformed 3DSE-GRETA along the *ScanFish* transect during the first cycle, with large prediction errors in both cases, the cumulative impact of the observations guided through the adaptive sampling procedure allowed to improve the prediction compared to 3DSE-LAURA and to reduce the mean forecast error by a factor three.

The temperature predictions along the *ScanFish* transect during this last forecast cycle are illustrated in Fig. 7. Even if none of the simulations properly predicts the fine-scale spatio-temporal variability of the thermocline, 3DSE-GRETA provides a more accurate mean representation of the measured field. The ocean temperature is underestimated by 3DSE-LAURA prediction along the westernmost part of the transect, while it is overestimated in the final part. A satellite SST image available on 25 August at 20:03 (i.e. during the last sampling cycle) indicates that the position of the thermal front has moved towards the coast associated with a northward spreading of warm coastal waters compared to the situation on 22 August (Fig. 1). This means that while *LAURA* was monitoring the cold side of the front during the last sampling period, *GRETA* was experiencing warmer waters to the north. One consequence is that the thermal front is pushed towards the coast in 3DSE-LAURA prediction with increased cross-frontal gradients. The *ScanFish* transect, which crosses this predicted position of the thermal front approximately aligned with the 500 m isobath, does not reveal any significant horizontal temperature gradient, thus evidencing the misplacement of the front in 3DSE-LAURA prediction. Meanwhile, the adaptive-sampling-driven simulation provides a more homogeneous temperature estimate along the transect, which better corresponds to the measured field.

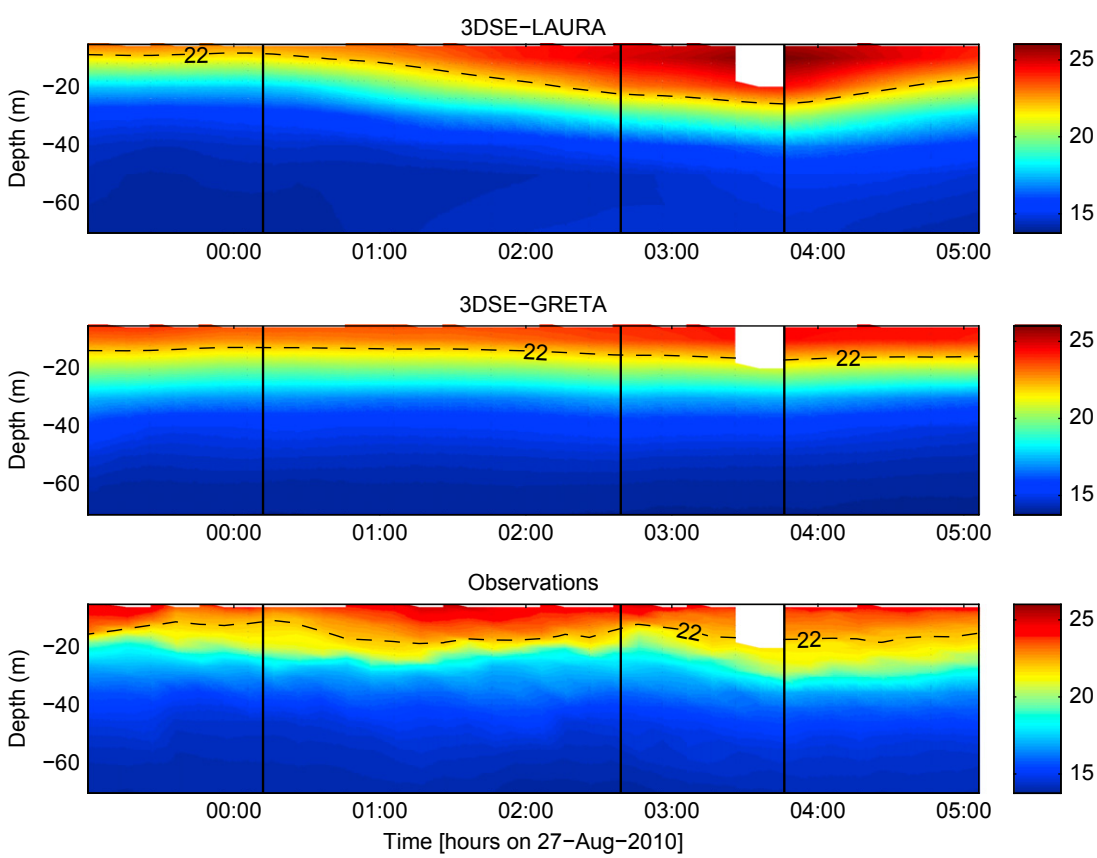

Fig. 7. Vertical temperature sections (°C) along the *ScanFish* transect between 26 August 2010 23:00 and 27 August 2010 05:00. Up: 3DSE-LAURA; middle: 3DSE-GRETA; bottom: observations from the *ScanFish*. The dashed lines show the position of the 22 °C isotherm. The black vertical lines indicate the change of direction of the instrument. The full transect, which starts from its westernmost position, is represented on the bottom-right panel in Fig. 6.

4. Summary and conclusions

The autonomous capability of ocean gliders allows a cost-effective way of increasing the spatial and temporal coverage of oceanic profile observations since the two-way communication system allows to pilot them in real time along targeted trajectories. This makes adaptive sampling a very appealing procedure to improve model ocean predictions by real time assimilation of the collected measurements. The benefit of adaptive sampling was previously demonstrated in purely numerical experiments (e.g. Zhang et al., 2010a,b). However, operational constraints and uncertainties associated with model predictions may lead to significant inconsistencies between the expected and the actual advantages of the procedure in real time exercises. The assessment of the real benefits of adaptive sampling with a single glider requires (i) at least one simultaneous "non-adaptive" sampling of the area with a similar instrument under the same geographical and operational constraints, and (ii) a large amount of observations to evaluate the skills of the associated forecasts. Such an assessment was presented in this paper, based on (i) the measurements collected during the REP10 sea trial held in the Ligurian Sea in August 2010, and (ii) the ocean temperature and velocity predictions by the 3DSE model run operationally during the experiment.

The benefit of adaptive sampling was assessed by comparing two 3DSE model simulations run operationally during the REP10 sea trial. While the first simulation was assimilating data from a glider guided by an adaptive sampling strategy, the second one incorporated data from a second glider that followed independent sampling objectives. Both *SLOCUM* gliders were equipped with similar CTD instruments, and were constrained to operate in the same area. For the glider undertaking adaptive sampling, a glider mission was planned to minimize the depth-integrated temperature uncertainty predicted by the 3DSE model during a 48-h forecast period.

The operational experiment demonstrated that the glider piloting algorithm, which re-directs the glider at each surfacing to compensate for the drift due to un-predicted currents, was able to properly guide the platform along the planned trajectory. Nevertheless, the glider was also found to require more time to complete the optimal paths than the transect time estimated from the glider nominal speed corrected by the forecasted ocean velocities. Adverse currents, which were not properly predicted by the model, were experienced along the glider path. The univariate formulation of the 3DSE method, together with the lack of ocean velocity observations to be assimilated, made the prediction of ocean currents particularly inaccurate in this experiment. Due to the slow motion of the platform, the feasibility of the trajectories obtained from the glider mission planner strongly depends on the accuracy of ocean current estimates. The effect of these ocean current prediction errors should be taken into account when improving future glider mission planners, for instance by artificially limiting the length of the planned trajectories.

The uncertainty predicted by the 3DSE model was found to be progressively reduced after each 48-h simulation cycle. During the last cycle, the uncertainty was 55% smaller when assimilating observations from the adaptive sampling than when assimilating data from the alternative path, showing that the adaptive sampling procedure implemented in this exercise was able to properly meet the proposed objective in a fully operational framework.

The underlying purpose associated with the reduction of the predicted model uncertainty is the improvement of the model forecast skill, characterized by a reduction of the actual prediction error computed against *in situ* measurements. The consistency between the predicted uncertainty and the actual mismatch with observations is related to the model capability to accurately predict the uncertainty associated with a given forecast. This capability is fundamental to conduct efficient adaptive sampling exercises based on model error reduction. Therefore, research concerning the evaluation and quantification of model uncertainties (e.g. Gawarkiewicz et al., 2011; Mourre et al., 2012) is needed in parallel to improvements in glider path planning accounting for poorly predicted dynamic ocean currents (e.g. Lolla et al., in press) to improve the overall performance of glider adaptive sampling.

The assessment of model predictions in such oceanic regions characterized by a significant small-scale variability in both space and time is inherently limited by the sparsity of *in situ* observations available for validation. Nevertheless, the time series at ODAS mooring, the repetition of a *ScanFish* transect in the central part of the domain and the presence of more randomly distributed observations over the study area provided a valuable dataset to evaluate the benefit of the adaptive sampling in the REP10 scenario. The prediction error was reduced at ODAS mooring over the whole 6-day experiment period when assimilating the observations from the adaptive sampling compared to the alternative glider. The prediction error was also reduced by a factor three along the final *ScanFish* transect compared to the initial one, with a better final performance of the adaptive-sampling-driven prediction over the control forecast. Finally, the cumulative effect of the observations guided through adaptive sampling over the three cycles contributed to improve the model prediction during the last validation period. Thus, even if the available dataset prevented the proper characterization of the spatio-temporal variability of the prediction error, it provided coherent indices that the 3DSE forecast better represented the true ocean field when assimilating data from the glider piloted via the adaptive sampling procedure. Quantitatively, the total RMSD against observations scattered over the modeling area during the last cycle was 18% lower for the model prediction integrating the data from the adaptive sampling compared to the control prediction. This demonstrates the benefit of the feedback of information between the observational platform and the numerical prediction system.

One of the lessons learnt from this exercise is that the multivariate assimilation of glider data should be considered to reduce the uncertainty associated with the ocean currents faced by the platforms so as to better generate timely reachable trajectories. Moreover, the accuracy of the 3DSE temperature predictions was shown to rapidly drop in this experiment when increasing the distance to the assimilated observations, making a large amount of data necessary to properly train the 3DSE model over an extended area. This probably limited the model prediction capability in this study due to the exclusive assimilation of *GRETA* or *LAURA* glider data below the surface in order to reserve a sufficient amount of independent observations for the forecast validation. In this regard, the consideration of a fleet of gliders guided though adaptive sampling may contribute to reduce the overall 3DSE prediction error in future experiments.

Finally, let us point out that the evaluation of the operational adaptive sampling methodology presented in this paper remains dependent on (i) the area under study, (ii) the data assimilative model used to predict ocean temperature and currents and their uncertainties and (iii) the particular "non-adaptive" or control glider path available to provide a comparison to the adaptive sampling scenario. These dependencies, which are inevitably linked to the required selection of experimental parameters, should encourage further real time adaptive sampling experiments and demonstrations of benefits in different oceanographic and modeling environments.

Acknowledgments

We would like to thank the Naval Research Laboratory (NRL-SSC) and PREVIMER for providing ocean forecasts used as input for the

3DSE. We are grateful to Chuck Trees for leading the REP10 experiment, Jacopo Chiggiato for running ROMS simulations at NURC, and Daniele Cecchi, Giuliana Pennucci, Gisella Baldasserini, Craig Lewis, Matt Cofin and Domencio Galletti for piloting the gliders during the experiment. We acknowledge the EuroSITES Project for providing data collected at ODAS Italia 1 observatory. This work was funded by the North Atlantic Treaty Organization. We thank the three anonymous reviewers for their time and careful and constructive reviews of the manuscript.

References

Alvarez, A., Caiti, A., Onken, R., 2004. Evolutionary path planning for autonomous underwater vehicles in a variable ocean. IEEE J. Oceanic Eng. 29 (2), 418–429.

Alvarez, A., Reyes, E., 2010. Volumetric estimation of thermal fields inferred from glider-like and remote sensing measurements in under-sampled coastal regions. J. Geophys. Res. 115, C11006.

Alvarez, A., Mourre, B., 2012. Optimal sampling designs for a glider-mooring observing network. J. Atmos. Oceanic Technol. 29 (4), 601–612.

Bouffard, J., Pascual, A., Ruiz, S., Faugère, Y., Tintoré, J., 2010. Coastal and mesoscale dynamics characterization using altimetry and gliders: a case study in the Balearic Sea. J. Geophys. Res. 115, C10029.

Castelao, R., Glenn, S., Schoefiled, O., Chant, R., Wilkin, J., Kohut, J., 2008. Seasonal evolution of hydrographic fields in the central MIddle Atlantic Bight from glider observations. Geophys. Res. Lett. 35 (3), L03617.

Chao, Y., Li, Z., Farrara, J.D., Moline, M.A., Schofield, O.M.E., Majumdar, S.J., 2008. Synergistic applications of autonomous underwater vehicles and the regional ocean modeling system in coastal ocean forecasting. Limnol. Oceanogr. 53, 2251–2263.

Chao, Y., Li, Z., Farrara, J., McWilliams, J.C., Bellingham, J., Capet, X., Chavez, F., Choi, J.-K., Davis, R., Doyle, J., Frantaoni, D., Li, P.P., Marchesiello, P., Moline, M.A., Paduan, J., Ramp, S., 2009. Development, implementation and evaluation of a data-assimilative ocean forecasting system off the central California coast. Deep-Sea Res. II 56, 100–126.

Cummings, J., 2005. Operational multivariate ocean data assimilation. Q. J. R. Meteorol. Soc. 131, 3583–3604.

Curtin, T., Bellingham, J., Catipovic, J., Webb, D., 1993. Autonomous oceanographic sampling networks. Oceanography 6 (3), 86–94.

Davis, R.E., Ohman, M.D., Rudnick, D.L., Sherman, J.T., Hodges, B., 2008. Glider surveillance of physics and biology in the southern California Current System. Limnol. Oceanogr. 53 (5 (Part 2)), 2151–2168.

Dobricic, S., Pinardi, N., Testor, P., Send, U., 2010. Impact of data assimilation of glider observations in the Ionian Sea (Eastern Mediterranean). Dyn. Atmos. Oceans 50 (1), 78–92.

Fiorelli, E., Leonard, N.E., Bhatta, P., Paley, D., Bachmayer, R., Fratantoni, D., 2004. Multi-AUV Control and adaptive sampling in Monterey Bay. In: IEEE/OES Autonomous Underwater Vehicles. pp. 134–147.

Gawarkiewicz, G., Jan, S., Lermusiaux, P.F.J., McClean, J.L., Centurioni, L., Taylor, K., Cornuelle, B., Duda, T.F., Wang, J., Yang, Y.J., Sanford, T., Lien, R.-C., Lee, C., Lee, M.-A., Leslie, W., Haley Jr., P.J., Niiler, P.P., Gopalakrishnan, G., Velez-Belchi, P., Lee, D.-K., Kim, Y.Y., 2011. Circulation and intrusions northeast of Taiwan: chasing and predicting uncertainty in the cold dome. Oceanography 24 (4), 110–121.

Haidvogel, D.B., Arango, H., Budgell, W.P., Cornuelle, B.D., Curchitser, E., Di Lorenzo, E., Fennel, K., Geyer, W.R., Hermann, A.J., Lanerolle, L., Levin, J., McWilliams, J.C., Miller, A.J., Moore, A.M., Powell, T.M., Shchepetkin, A.F., Sherwood, C.R., Signell, R.P., Warner, J.C., Wilkin, J., 2008. Ocean forecasting in terrain-following coordinates: formulation and skill assessment of the Regional Ocean Modeling System. J. Comput. Phys. 227, 3595–3624.

Haley, P., Lermusiaux, P., Robinson, A., Leslie, W., Logutov, O., Cossarini, G., Liang, X., Moreno, P., Ramp, S., Doyle, J., Bellingham, J., Chavez, F., Johnston, S., 2009. Forecasting and reanalysis in the Monterey Bay/California Current region for the Autonomous Ocean Sampling Network-II experiment. Deep-Sea Res. II 56, 127–148.

Heaney, K.D., Gawarkiewicz, F., Lermusiaux, P.F.J., 2007. Non-linear optimization of autonomous undersea vehicle sampling strategies for oceanographic data-assimilation. J. Field Rob. 24 (6), 437–448. (Special Issue on Underwater Robotics).

Hooke, R., Jeeves, T.A., 1961. Direct search solutions of numerical and statistical problems. J. Assoc. Comput. Mach. 8, 212–229.

Lazure, P., Dumas, F., 2008. An external-internal mode coupling for a 3D hydrodynamical model for applications at regional scale (MARS). Adv. Water Resour. 31, 233–250.

Lenartz, F., Mourre, B., Barth, A., Beckers, J.-M., Vandenbulcke, L., Rixen, M., 2010. Enhanced ocean temperature forecast skills through 3-D super-ensemble multi-model fusion. Geophys. Res. Lett. 37 (19), L19606.

Leonard, N.E., Paley, D.A., Lekien, F., Sepulchre, R., Fratantoni, D.M., Davis, R.E., 2006. Collective motion, sensor networks and ocean sampling. Proc. IEEE 95 (1), 48–74.

Leonard, N.E., Paley, D.A., Davis, R.E., Fratantoni, D.M., Lekien, F., Zhang, F., 2010. Coordinated control of an underwater glider fleet in an adaptive ocean sampling field experiment in Monterey Bay. J. Field Rob. 27 (6), 718–740.

Lermusiaux, P.F.J., 2007. Adaptive modeling, adaptive data assimilation and adaptive sampling. Physica D 230, 172–196.

Lolla, T., Ueckermann, M.P., Yigit, K., Haley, P., Lermusiaux, P.F.J. Path planning in time dependent flow fields using level set methods. In: IEEE International Conference on Robotics and Automation, in press.

McIntosh, P.C., 1990. Oceanographic data interpolation: objective analysis and splines. J. Geophys. Res. 95, 13529–13541.

Martin, P.J., 2000. Description of the Navy Coastal Ocean Model Version 1.0. NRL/FR/7322-00-9962. Naval Research Laboratory. 42 pp.

Mourre, B., Chiggiato, J., Lenartz, F., Rixen, M., 2012. Uncertainty forecast from 3-D super-ensemble multi-model combination: validation and calibration. Ocean Dyn. 62 (2), 283–294.

Ramp, S., Davis, R., Leonard, N., Shulman, I., Chao, Y., Robinson, A., Marsden, J., Lermusiaux, P., Fratantoni, D., Paduan, J., Chavez, F., Bahr, F., Liang, S., Leslie, W., Li, Z., 2009. Preparing to predict: the second autonomous ocean sampling network (AOSN-II) experiment on the Monterey Bay. Deep-Sea Res. II 56, 68–87.

Ramp, S., Lermusiaux, P., Shulman, I., Chao, Y., Wolf, R., Bahr, F., 2011. Oceanographic and atmospheric conditions on the continental shelf north of the Monterey Bay during August 2006. Dyn. Atmos. Oceans 52, 192–223.

Robinson, A.R., Glenn, S.M., 1999. Adaptive sampling for ocean forecasting. Naval Res. Rev. 51 (2), 28–38.

Ruiz, S., Pascual, A., Garau, B., Faugère, Y., Alvarez, A., Tintoré, J., 2009. Mesoscale dynamics of the Balearic Front, integrating glider, ship and satellite data. J. Marine Syst. 78, S3–S16.

Smith, R.N., Chao, Y., Li, P.P., Caron, D.A., Jones, B.H., Sukhatme, G.S., 2010. Planning and implementing trajectories for autonomous underwater vehicles to track evolving ocean processes based on predictions from a regional ocean model. Int. J. Rob. Res. 29 (12), 1475–1497.

Stark, D.J., Donlon, C.J., Martin, M.J., McCulloch, M.E., 2007. OSTIA: an operational, high resolution, real time, global sea surface temperature analysis system. In: Marine Challenges: Coastline to Deep Sea. Oceans 07 IEEE Aberdeen, Conference Proceedings. IEEE, Aberdeen, Scotland.

Stein, L.M., 1999. Interpolation of Spatial Data. Springer-Verlag, New York 246 pp..

Todd, R.E., Rudnick, D.L., Davis, R.E., Ohman, M.D., 2011. Underwater gliders reveal rapid arrival of El Nio effects off California's coast. Geophys. Res. Lett. 38 (3), L03609.

Wang, D., Lermusiaux, P.F.J., Haley, P.J., Eickstedt, D., Leslie, W.G., Schmidt, H., 2009. Acoustically focused adaptive sampling and on-board routing for marine rapid environmental assessment. J. Mar. Syst. 78, S393–S407.

Yilmaz, N.K., Evangelinos, C., Lermusiaux, P.F.J., Patrikalakis, N., 2008. Path planning of autonomous underwater vehicles for adaptive sampling using mixed integer linear programming. IEEE J. Oceanic Eng. 33 (4), 522–537.

Zhang, W.G., Wilkin, J.L., Arango, H.G., 2010a. Towards building an integrated observation and modeling system in the New York Bight using variational methods. Part I. 4DVAR data assimilation. Ocean Modelling 35, 119–133.

Zhang, W.G., Wilkin, J.L., Levin, J.C., 2010b. Towards building an integrated observation and modeling system in the New York Bight using variational methods. Part II. Representer-based observing system evaluation. Ocean Modelling 35, 134–145.

Document Data Sheet

Security Classification		Project No.
Document Serial No.	**Date of Issue**	**Total Pages**
CMRE-PR-2014-006	January 2014	11 pp.

Author(s)

Mourre, B., Alvarez, A.

Title

Benefit assessment of glider adaptive sampling in the Ligurian Sea.

Abstract

The benefits of piloting a glider during a 6-day period via an adaptive sampling procedure in a 80 × 60 km^2 marine area are assessed under a fully operational framework. The glider trajectory was adapted to reduce the ocean temperature uncertainties predicted by the operational 3-D super- ensemble model in the Ligurian Sea in August 2010. Two sets of real time model predictions are compared, which assimilate observations from (1) the adaptive-sampling-driven glider and (2) an independent glider flying in the same area. The piloting algorithm was able to successfully guide the glider along the planned trajectories. These were nevertheless not fully completed due to un-predicted adverse currents faced along the transects. Despite operational constraints and model prediction errors, the adaptive sampling procedure is shown to meet the proposed objective, i.e. a reduction of the 48-h model temperature uncertainty predicted in the upper 200 m. Moreover, measurements collected during the last 48-h forecast cycle from (i) an ocean mooring, (ii) a repeated ScanFish transect and (iii) more irregularly distributed platforms, all indicate that the actual prediction error is lower in the simulation assimilating the data from the adaptive sampling. Quantitatively, the total root-mean- square error is reduced by18% at the end of the field experiment in comparison with the control simulation.

Keywords

Issuing Organization

Science and Technology Organization
Centre for Maritime Research and Experimentation

Viale San Bartolomeo 400, 19126 La Spezia, Italy

[From N. America:
STO CMRE
Unit 31318, Box 19, APO AE 09613-1318]

Tel: +39 0187 527 361
Fax:+39 0187 527 700

E-mail: library@cmre.nato.int